



**HAL**  
open science

## 1,3 Dioxolane versus tetrahydrofuran as promoters for CO<sub>2</sub>-hydrate formation: Thermodynamics properties, and kinetics in presence of sodium dodecyl sulfate

Jean-Philippe Torre, Didier Haillet, Sacha Rigal, Roger de Souza Lima, Christophe Dicharry, Jean-Pierre Bedecarrats

### ► To cite this version:

Jean-Philippe Torre, Didier Haillet, Sacha Rigal, Roger de Souza Lima, Christophe Dicharry, et al.. 1,3 Dioxolane versus tetrahydrofuran as promoters for CO<sub>2</sub>-hydrate formation: Thermodynamics properties, and kinetics in presence of sodium dodecyl sulfate. *Chemical Engineering Science*, 2015, 126, pp.688-697. 10.1016/j.ces.2015.01.018 . hal-01279226

**HAL Id: hal-01279226**

**<https://hal.science/hal-01279226>**

Submitted on 8 Feb 2019

**HAL** is a multi-disciplinary open access archive for the deposit and dissemination of scientific research documents, whether they are published or not. The documents may come from teaching and research institutions in France or abroad, or from public or private research centers.

L'archive ouverte pluridisciplinaire **HAL**, est destinée au dépôt et à la diffusion de documents scientifiques de niveau recherche, publiés ou non, émanant des établissements d'enseignement et de recherche français ou étrangers, des laboratoires publics ou privés.




## Open Archive Toulouse Archive Ouverte

OATAO is an open access repository that collects the work of Toulouse researchers and makes it freely available over the web where possible

This is an author's version published in: <http://oatao.univ-toulouse.fr/21626>

**Official URL:** <https://doi.org/10.1016/j.ces.2015.01.018>

### To cite this version:

Torré, Jean-Philippe  and Haillet, Didier and Rigal, S. and de Souza Lima, Roger and Dicharry, Christophe and Bedecarrats, Jean-Pierre *1,3 Dioxolane versus tetrahydrofuran as promoters for CO<sub>2</sub>-hydrate formation: Thermodynamics properties, and kinetics in presence of sodium dodecyl sulfate.* (2015) *Chemical Engineering Science*, 126. 688-697. ISSN 0009-2509

Any correspondence concerning this service should be sent to the repository administrator: [tech-oatao@listes-diff.inp-toulouse.fr](mailto:tech-oatao@listes-diff.inp-toulouse.fr)

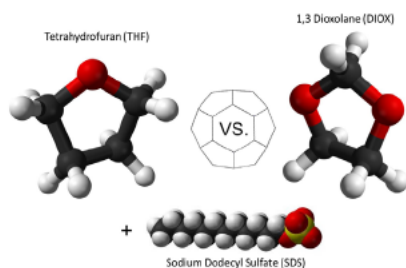
# 1,3 Dioxolane versus tetrahydrofuran as promoters for CO<sub>2</sub>-hydrate formation: Thermodynamics properties, and kinetics in presence of sodium dodecyl sulfate

J.-P. Torr <sup>a,\*</sup>, D. Haillot<sup>b</sup>, S. Rigal<sup>b</sup>, Roger de Souza Lima<sup>b</sup>, C. Dicharry<sup>a</sup>, J.-P. Bedecarrats<sup>b</sup>

<sup>a</sup> Univ. Pau & Pays Adour, CNRS, TOTAL–UMR 5150–LFC–R–Laboratoire des Fluides Complexes et leurs R servoirs, Avenue de l'Universit , BP 1155, Pau F-64013, France

<sup>b</sup> Univ. Pau & Pays Adour, EA1932–LaTEP–Laboratoire de Thermique Energ tique et Proc d s, Rue Jules Ferry, BP 7511, Pau F-64075, France

- Search for efficient and easy to use promoters for clathrate hydrate formation.
- Experimental results obtained by using high pressure calorimetry and a batch reactor.
- Data on hydrate phase equilibrium and kinetics obtained using DIOX, THF, and SDS.
- The combination of THF or DIOX with SDS speeds up enclathration.
- THF, used alone or with SDS, is a more effective hydrate promoter than DIOX.



## A B S T R A C T

This paper makes a comparison between tetrahydrofuran (THF) and 1,3 dioxolane (DIOX) in terms of their respective performances as promoters for the formation of clathrate hydrates with CO<sub>2</sub>. The aim is to find products that can be substituted for THF, which is known to be harmful and difficult to handle. Drawing on a review of the chemical and physical properties of these two organic compounds, experiments were performed using high pressure differential scanning calorimetry (DSC) and a batch reactor. Details of the thermodynamic equilibria of mixed THF+CO<sub>2</sub> and DIOX+CO<sub>2</sub> hydrates obtained with various additive concentrations are provided, along with hydrate kinetics data relating to the hydrate formation. The effect of the presence of an anionic surfactant, SDS (sodium dodecyl sulfate), on hydrate formation kinetics was also evaluated, showing that a combination of THF or DIOX and SDS is a very advantageous solution for accelerating hydrate formation. THF has been found to outperform DIOX as a hydrate promoter from both a thermodynamic, and a kinetic standpoint in presence of SDS. However, DIOX remains an interesting practical solution, due to the benefits offered as the least toxic and aggressive of these two organic compounds.

**Keywords:**  
Gas hydrate  
Clathrate  
Additive  
Equilibrium data  
SDS  
CO<sub>2</sub>

## 1. Introduction

Clathrate hydrates (named hydrates in the following) are ice like crystalline compounds consisting of a lattice structure formed by a

network of water molecules which, under certain thermodynamic conditions, can engage individual small guest molecules of suitable size and shape (Sloan, 2003). Hydrates crystallize with different structures; the two most common ones encountered in nature or in laboratories are structures one (sI) and two (sII) (Jeffrey, 1984). Many details and properties of these compounds can be found elsewhere in the literature on this subject (Sloan and Koh, 2008). In addition,

\* Corresponding author. Tel.: +33 5 40 17 51 09.

E-mail address: jean-philippe.torre@univ-pau.fr (J.-P. Torr ).

hydrates are currently the subject of intensive research studies aimed at using these compounds in various promising applications such as gas separation processes (Eslamimanesh et al., 2012; Zhong et al., 2013), sea water desalination (Wang et al., 2013) and refrigeration (Delahaye et al., 2008). In some cases, the application calls for some fine tuning of the hydrate formation conditions (e.g., the formation pressure has to be reduced and/or the formation temperature increased) or a boost to the kinetic mechanisms of hydrate formation. For this purpose it is common for chemical additives, called hydrate promoters, to be added to the water. Among the various chemical compounds able to act as hydrate promoters, tetrahydrofuran (THF) and 1,3 dioxolane (DIOX) can be used. Some of the main relevant properties of these two organic compounds and their clathrate hydrates are summarized in Table S1 in Supplementary information. THF is probably one of the most popular hydrate thermodynamic promoter and its efficiency has been already tested and demonstrated for many systems. DIOX, a cyclic ether like THF, is a potential candidate as hydrate promoters, much less studied than THF, but with some interesting properties and advantages which will be detailed in the following.

THF is a volatile and extremely flammable substance, with a characteristic ether like odor, which can form peroxides if stored with long exposure to air (Uchida et al., 2008). In addition, it is a severe eye irritant and a mild skin irritant (Arnett et al., 1995). The use of THF in laboratory experiments can also be responsible for technical problems with apparatuses and/or analytical devices, essentially due to its highly aggressive action on some plastics, rubbers, and coatings (e.g., seals, valves, O rings, etc.) (Mackison et al., 1981). In appropriate temperature conditions, THF and water form the so called "THF hydrate" with formula THF  $17\text{H}_2\text{O}$ , which melts congruently at around 277 K and in which THF molecules occupy only the large cages of the structure (sII). Detailed information about the full THF water phase diagram can be found elsewhere in the literature (Makino et al., 2005). In addition, THF is known to act as a powerful gas hydrate promoter, as it allows mixed gas hydrates (i.e., hydrates containing both THF and gas, for example THF +  $\text{CO}_2$  hydrate) to form at significantly lower pressure and higher temperature than the hydrate formed without this promoter ( $\text{CO}_2$  hydrate in this case) (Delahaye et al., 2006). This promoting effect has been demonstrated in the presence of various gases (such as  $\text{CO}_2$ ,  $\text{N}_2$ ,  $\text{CH}_4$ ,  $\text{H}_2$ ) and several gas mixtures (such as  $\text{CO}_2 + \text{CH}_4$ ,  $\text{CO}_2 + \text{N}_2$ ) (Anderson et al., 2007; Kang et al., 2001; Lee et al., 2012). Interestingly, it was demonstrated that using this kind of thermodynamic promoter in combination with an anionic surfactant such as sodium dodecyl sulfate (SDS) can considerably enhance hydrate crystallization in quiescent conditions (Lirio et al., 2013; Ricaurte et al., 2014a), or in porous media (Dicharry et al., 2013; Yang et al., 2013), and even using a very low dose of THF (Ricaurte et al., 2014b).

DIOX is also a flammable liquid, but is less volatile than THF, and with a sweet odor detectable at a higher concentration in air than for THF (see Table S1 in Supplementary information). Like other ethers such as THF and ethyl ether, DIOX forms peroxides on exposure to air (Uchida et al., 2008); however, it does not seem to accumulate them to dangerously high levels (BASF, 2013). Regarding the toxicological information presented in Table S1 (i.e., the median lethal dose  $\text{LD}_{50}$  (absorption), the medial lethal concentration  $\text{LC}_{50}$  (inhalation) and the NFPA index), DIOX is less harmful than THF (NFPA (National Fire Protection Association), 2010, 2002). DIOX forms also a clathrate of structure (sII), of formula DIOX  $17\text{H}_2\text{O}$  and it proved possible to unearth data on the static dielectric constant (Venkatesjvara et al., 1967) and on thermal properties (Ahmad and Phillips, 1987; Andersson and Ross, 1983; Yonekura et al., 1995), along with a diagram of a solid liquid phase obtained with mixtures of THF and DIOX (Nakayama and Hashimoto, 1980). Concerning mixed DIOX hydrates, only results obtained with methane (de Deugd et al., 2001) and Xenon

(Maekawa, 2013) were found, which demonstrates that DIOX works as a hydrate promoter with these gases.

Very surprisingly, although DIOX and THF have fairly similar molecular structures, and DIOX has been proposed by chemical companies (e.g., BASF) as a solvent/reactant that would be an attractive alternative to THF, very few studies concerning clathrate hydrates formed with this molecule have been published, and very little information (e.g., on thermodynamic data, influence on crystallization kinetics, spectroscopic characterization) is available in the literature. Finding suitable products that can be substituted for THF, and characterizing to what extent the proposed molecules can be used for hydrate based applications, are therefore of great importance. In this respect, this paper makes a detailed comparison between THF and DIOX as hydrate promoters, comparing the equilibrium data and hydrate formation kinetics data obtained with pure  $\text{CO}_2$  (with and without SDS), and factoring in safety considerations and physical/chemical properties.

## 2. Experimental apparatuses and materials

### 2.1. High pressure differential scanning calorimeter

Hydrate formation/dissociation studies were performed using a high pressure differential scanning calorimeter (micro DSC VII from Setaram). It is based on a symmetrical heat flux design, according to the Calvet principle (le Parlouër et al., 2004). It operates between 228 and 393 K thanks to Peltier thermoelectric devices, with uncertainty estimated at 0.2 K. Heating and cooling rates are between 0.001 and 2  $\text{K min}^{-1}$ , and measurements can be performed at up to 25.0 MPa. The volume of the measurement and reference gas tight high pressure cells is 1  $\text{cm}^3$ . The cells are placed inside the calorimetric block and connected to a gas controlled panel which contains a 300  $\text{cm}^3$  vessel to maintain a constant pressure in the measurement cell. During the experiment, pressure is measured using a pressure transducer with uncertainty estimated at  $\pm 0.05$  MPa.

### 2.2. Experimental rig for kinetic experiments

Hydrates are formed in a batch jacketed reactor able to perform experiments at pressures of up to 20 MPa and temperatures ranging from 263 to 323 K. Two lateral sapphire windows allow the inside of the reactor to be observed during the experiment. For gas solubilization, the cell is equipped with a star shaped magnetic agitator, driven by a magnetic stirrer located below the cell. Note that this agitation system is unable to stir any hydrate slurry, which means that hydrates growth under "quiescent conditions". The volume of the reactor is  $168.0 \pm 0.9 \text{ cm}^3$ , and the temperature is measured by a PT100 with an accuracy of  $\pm 0.2$  K. The reactor pressure is measured with a 0–10 MPa pressure transmitter (PA33X from KELLER) with an accuracy of  $\pm 0.02$  MPa. Snapshots are extracted from videos recorded by a conventional webcam (LiveCam Optia AF from Creative Labs). Data acquisition takes place with a frequency of 1 Hz. More technical details and a diagram of the apparatus are given in another work (Torré et al., 2012).

### 2.3. Materials

Information about the materials used for the experiments (CAS numbers, purity and suppliers) has been collated and is given in Table 1. The gas used was carbon dioxide ( $\text{CO}_2$ ), and initial solutions were prepared using ultra pure water with a resistivity of 18.2  $\text{M}\Omega \text{ cm}$ . SDS is only present in the kinetics experiments.

### 3. Protocols and methods of the experiments

#### 3.1. Protocol for calorimetry experiments

Once prepared, approximately 80 mg of a THF/water or DIOX/water solution is introduced into the measurement cell of the high pressure calorimeter. It is then connected to the high pressure controlled panel. In order to expel the air initially present in the cell and avoid any loss of the volatile compound (THF or DIOX), the sample is first crystallized at low temperature (248 K) and then three purges are performed using CO<sub>2</sub>.

The reference cell is carefully filled with nitrogen, which does not undergo any physical or chemical change at the pressure and temperature of the experiments. The formation of mixed hydrates (i. e., THF+CO<sub>2</sub> or DIOX+CO<sub>2</sub>) compete with the possible formation of metastable phases (e.g., ice and THF or DIOX hydrates [Martinez et al., 2008](#)), and the formation of single hydrates of CO<sub>2</sub>. To enhance the mixed hydrate formation, the sample is subjected to a series of heating and cooling sequences whose final temperatures are adjusted. The objective of these cycles is both to reduce the quantity of metastable phases at low temperature and to achieve a progressive accumulation of the desired compound (i.e., the mixed hydrate here) in the cell, until the final heating ramp during which the hydrate dissociation temperature is measured. An example of a thermogram, obtained for a sample containing 10.0 wt% THF, is plotted in [Fig. 1](#).

This experiment has ten heating/cooling cycles and a final heating sequence. During the cycle, heating and cooling rates are set to 2 K min<sup>-1</sup>. The last heating run was conducted with a slower rate (0.1 K min<sup>-1</sup>) until dissociation of the hydrate was complete. It highlights two endothermic peaks: the first peak (marked with a single asterisk in [Fig. 1](#)) is related to the dissociation of the CO<sub>2</sub> hydrate, and the second (marked with a double asterisk in [Fig. 1](#)) is a progressive

**Table 1**

Materials CAS numbers, purity and suppliers; superscripts <sup>a</sup> and <sup>b</sup> refer to phase equilibrium and kinetics experiments, respectively.

| Product         | CAS      | Purity (%) | Supplier  |
|-----------------|----------|------------|---|
| THF             | 109-99-9 | > 99.9     | Sigma Aldrich                                     |
| DIOX            | 646-06-0 | 99.5       | Alfa Aesar  |
| CO <sub>2</sub> | 124-38-9 | 99.995     | Air liquide <sup>a</sup> , Linde gas <sup>b</sup> |
| SDS             | 151-21-3 | > 99.8     | Chem-Lab  |

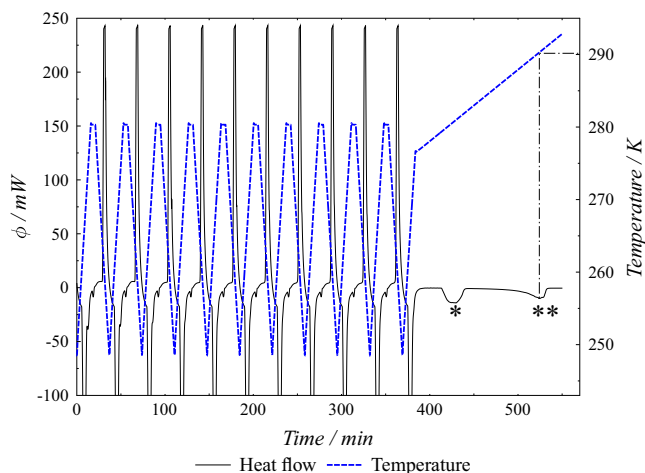


**Fig. 1.** Experimental protocol for hydrate formation and dissociation. HP-DSC typical experiment (10 temperature cycles followed by a final temperature ramp), with the H<sub>2</sub>O+THF 10.0 wt%)/CO<sub>2</sub> system, at 2.50 MPa of CO<sub>2</sub>. The \* symbol shows the dissociation of the CO<sub>2</sub> hydrate and the \*\* symbol shows the dissociation of THF+CO<sub>2</sub> mixed hydrate; the dot-dashed line shows how determine the dissociation temperature from the thermogram.

fusion peak relative to the dissociation of the THF+CO<sub>2</sub> mixed hydrate. The temperature pressure equilibrium points for the mixed hydrate correspond to the melting of the last hydrate crystal which is assumed to be at the top of the progressive dissociation peak, as proposed by [Delahaye et al. \(2006\)](#). As in the example presented here, DSC analysis performed at a CO<sub>2</sub> pressure of 2.5 MPa on the 10.0 wt% THF solution gives an equilibrium temperature equal to 290.1 ± 0.2 K, (as shown by the dot dashed line in [Fig. 1](#)).

#### 3.2. Protocol for kinetics experiments

As discussed in [Section 1](#), in addition to thermodynamic effects, the presence of THF and DIOX can also greatly influences the hydrate formation kinetics. In order to compare the effect of THF and DIOX and the effect of combining these additives with SDS, the same molar concentration (i.e., 1.0 mol%) has been used for THF and DIOX (corresponding to 4.0 wt% of THF and 4.1 wt% of DIOX). The SDS concentration was constant at 0.3 wt%.

The experiment protocol is as follows: first, a volume of 65 cm<sup>3</sup> of solution containing (or not) the additive(s) is loaded into the reactor. Then, the reactor and lines are purged three times with CO<sub>2</sub> to remove any trace of air in the system. It has been demonstrated in a previous work ([Ricaurte et al., 2012](#)) that with the concentration of organic additives used here, the loss of organic product during this step is negligible. The reactor is regulated at 293 K under agitation (600 RPM) and pressurized at 3.0 MPa. The pressure in the reactor is maintained constant under agitation for 120 min to solubilize the CO<sub>2</sub> in the solution. Note that the solubility equilibrium is reached in about 30 min (the pressure of the gas supply vessel reaches a constant value at the end of the solubilization process). At this point, the reactor is closed and the temperature decreased until the target temperature of 274.6 ± 0.2 K (suitable for hydrate formation) is reached. The system is then maintained at this temperature for at least 10 h. Finally, the reactor temperature is raised again to 293 K at a rate of 0.1 K min<sup>-1</sup> to dissociate the hydrate formed. For reproducibility reasons, note that all the experiments in this section have been performed four times for each condition and system studied.

#### 3.3. Methods and definition of kinetics variables

The calculations of the molar quantities of gas captured were performed using the Peng Robinson equation of state (PR EoS) ([Peng and Robinson, 1976](#)). To analyze quantitatively the enclathration kinetics, we have defined several additional variables (where the initial time  $t=0$  was set to the beginning of the reactor cooling phase):

When two successive hydrate crystallizations occur (e.g., the mixed hydrate first and then the CO<sub>2</sub> hydrate),  $t_1$  and  $t_2$  represent the times when the first and the second hydrate formations are measured, respectively.

$n_{\text{CO}_2}^{\text{capt}}$  is the total mol number of CO<sub>2</sub> captured at the point when time  $t$  equals 800 min.

$t_{90\%}$  is the time necessary to capture 90% of  $n_{\text{CO}_2}^{\text{capt}}$  (see [Fig. 2](#)).  $(dn/dt)|_{\text{max}}$  is the maximum CO<sub>2</sub> enclathration rate, obtained by numerical derivation of the quantity of CO<sub>2</sub> captured versus time (see [Fig. 2](#)).

$t_{(dn/dt)|_{\text{max}}}$  and  $P_{(dn/dt)|_{\text{max}}}$  are, respectively, the time and the reactor pressure when the enclathration rate is at its maximum.

## 4. Results and discussion

### 4.1. Thermodynamics

To validate the reliability of the experiment protocol defined in the previous section as a means of obtaining phase equilibrium

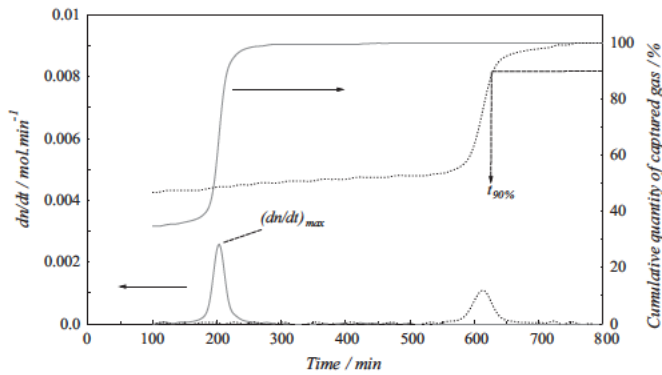


Fig. 2. Plots of the enclathration rate and the cumulative quantity of captured gas versus time. The method of determination of  $(dn/dt)_{max}$  and  $t_{90\%}$  are illustrated. The systems are: THF+SDS (full line) and DIOX+SDS (dashed line).

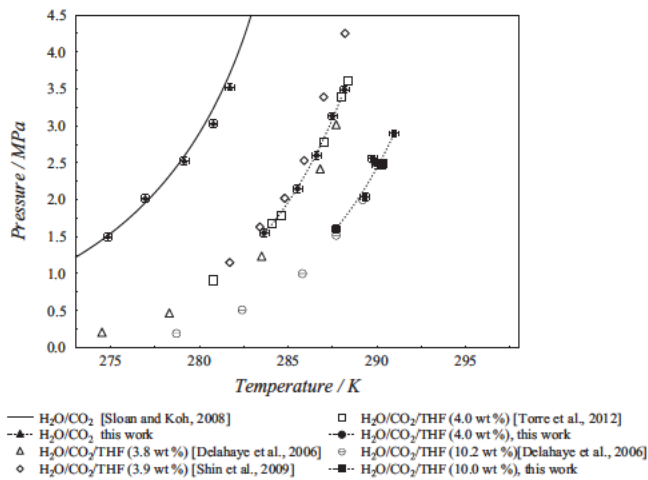


Fig. 3. Comparison between our DSC measurements and data set from literature:  $(T, P)$  equilibrium data of  $\text{CO}_2$  hydrates and of  $\text{CO}_2$ +THF mixed hydrates.

Table 2  
Experimental  $(T, P)$  equilibrium data of  $\text{CO}_2$ +THF mixed hydrates.

| $\text{H}_2\text{O}/\text{THF}$ (4.0 wt%)/ $\text{CO}_2$ |                 | $\text{H}_2\text{O}/\text{THF}$ (10.0 wt%)/ $\text{CO}_2$ |                 |
|--|-----------------|---|-----------------|
| $T$ (K)  | $P$ (MPa)       | $T$ (K)   | $P$ (MPa)       |
| $283.6 \pm 0.2$  | $1.55 \pm 0.05$ | $287.7 \pm 0.2$   | $1.61 \pm 0.05$ |
| $285.5 \pm 0.2$  | $2.15 \pm 0.05$ | $289.3 \pm 0.2$   | $2.04 \pm 0.05$ |
| $286.6 \pm 0.2$  | $2.60 \pm 0.05$ | $290.1 \pm 0.2$   | $2.50 \pm 0.05$ |
| $287.5 \pm 0.2$  | $3.13 \pm 0.05$ | $291.0 \pm 0.2$   | $2.90 \pm 0.05$ |
| $288.2 \pm 0.2$  | $3.49 \pm 0.05$ |   |                 |

data, a set of our DSC results was compared with those found in the literature. Fig. 3 illustrates the comparison between  $(T, P)$  equilibrium data of pure  $\text{CO}_2$  hydrates and of THF+ $\text{CO}_2$  mixed hydrates (initial THF concentrations of 4.0 and 10.0 wt%). Data obtained during our experiment campaign on the phase equilibrium of THF+ $\text{CO}_2$  mixed hydrates are given in Table 2.

Concerning  $\text{CO}_2$  hydrates, good consistency was observed between our data and those calculated using the CSMGem program (from Sloan and Koh, 2008). Our data on THF+ $\text{CO}_2$  mixed hydrates also seem to be corroborated by those of Delahaye et al. (2006) obtained with [THF]=3.8 and 10.2 wt%, those of Shin et al. (2009) with [THF]=3.9 wt%, and those of Torre et al. (2012) with [THF]=4.0 wt%. Accordingly, the presented protocol and method are validated. As expected, these results emphasize the thermodynamic promoting effect of THF, i.e., the equilibrium curve of the

mixed  $\text{CO}_2$ +THF hydrate is shifted to higher temperature for a given pressure compared to the equilibrium curve of the  $\text{CO}_2$  hydrate. As an example, the equilibrium point obtained at pressure 2.5 MPa with [THF]=4.0 and then 10.0 wt% is increased to 286.6 and 290.1 K, (respectively), compared with 279.1 K for pure  $\text{CO}_2$  hydrate at the same pressure.

The same protocol was used for water/DIOX/ $\text{CO}_2$  systems in order to assess the influence of DIOX on hydrate phase equilibrium. Two solutions containing DIOX at initial concentrations of 4.1 and 10.2 wt% were studied and compared against the results obtained with THF solutions of similar molar concentrations. Experimental results concerning the DIOX+ $\text{CO}_2$  mixed hydrate are plotted in Fig. 4, and the equilibrium data are summarized in Table 3.

For a given pressure, it is clearly apparent that the addition of DIOX in the same way as THF to water allows the mixed DIOX+ $\text{CO}_2$  hydrate to form at higher temperatures than those associated with the pure  $\text{CO}_2$  hydrate. This therefore demonstrates the effect of DIOX as a thermodynamic promoter. Nevertheless, a greater effect is achieved when THF is used. For instance, at a pressure of 2.5 MPa, the equilibrium temperature equals 290.1 and 283.2 K respectively with [THF]=10.0 wt% and [DIOX]=10.2 wt%. In conclusion, with the same molar concentration of additive, THF is a better thermodynamic promoter than DIOX.

#### 4.2. Kinetics

First, it is worth showing that the aqueous solutions containing THF or DIOX can behave very differently in the presence of  $\text{CO}_2$ , and these differences could be important for choosing the most suitable promoter in a practical situation. As preliminary studies,

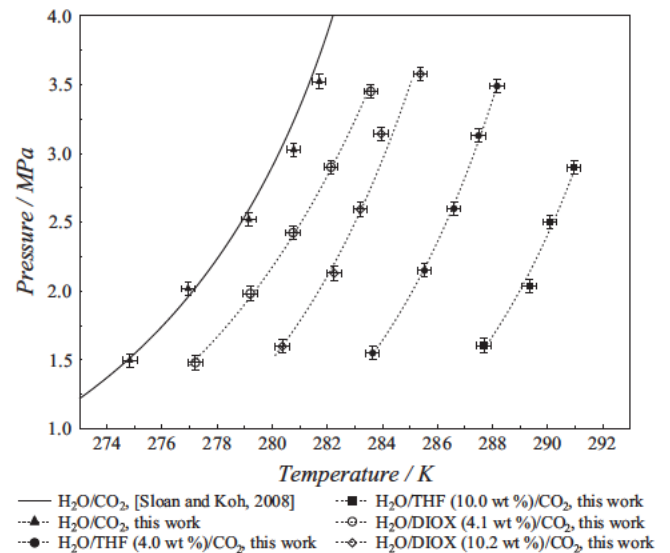


Fig. 4. Experimental  $(T, P)$  equilibrium data of  $\text{CO}_2$ +THF mixed hydrates ([THF] 4.0 and 10.0 wt%) and for  $\text{CO}_2$ +DIOX mixed hydrates ([DIOX] 4.1 and 10.2 wt%).

Table 3  
Experimental  $(T, P)$  equilibrium data of  $\text{CO}_2$ +DIOX mixed hydrates.

| $\text{H}_2\text{O}/\text{DIOX}$ (4.1 wt%)/ $\text{CO}_2$ |                 | $\text{H}_2\text{O}/\text{DIOX}$ (10.2 wt%)/ $\text{CO}_2$ |                 |
|---|-----------------|--|-----------------|
| $T$ (K)   | $P$ (MPa)       | $T$ (K)  | $P$ (MPa)       |
| $277.2 \pm 0.2$   | $1.48 \pm 0.05$ | $280.4 \pm 0.2$  | $1.60 \pm 0.05$ |
| $279.2 \pm 0.2$   | $1.98 \pm 0.05$ | $282.2 \pm 0.2$  | $2.13 \pm 0.05$ |
| $280.8 \pm 0.2$   | $2.42 \pm 0.05$ | $283.2 \pm 0.2$  | $2.59 \pm 0.05$ |
| $282.1 \pm 0.2$   | $2.90 \pm 0.05$ | $284.0 \pm 0.2$  | $3.14 \pm 0.05$ |
| $283.6 \pm 0.2$   | $3.45 \pm 0.05$ | $285.4 \pm 0.2$  | $3.58 \pm 0.05$ |

test runs were conducted in the reactor with the two systems at 293 K and CO<sub>2</sub> at 3.0 MPa. The concentrations for these tests are obtained based on the stoichiometric quantity of additive in water with respect to the (sII) hydrate formula G 17H<sub>2</sub>O, where G is THF or DIOX: the mass concentrations used are thus 19.2 wt% for THF and 19.6 wt% for DIOX. The observations made during the experiments are presented in Fig. 5.

As shown in Fig. 5(a) and (c), the initial solutions before CO<sub>2</sub> pressurization are monophasic. After CO<sub>2</sub> pressurization, it is clearly apparent in Fig. 5(b) that the water+THF system rapidly separates into two liquid phases, contrarily to the water+DIOX system which remains monophasic, as shown in Fig. 5(d). By way of consequence, for the water+THF system, a liquid layer rich in THF is formed at the top of the solution and can come into direct contact with the process equipment. The apparition of such an immiscible phase at this stage may be advantageous in some cases, for example if a THF water emulsion is desired. However, this “THF rich” layer is potentially damaging to the process equipment (e.g., the O rings of the reactor windows in our case), which are not resistant to this compound when it is used at such high concentrations. Process equipment can thus be damaged irreversibly in a short time, leading to potential hazardous leakages of flammable/toxic products (gas and/or liquid). Conversely, with the water+DIOX system, where no phase separation is observed when CO<sub>2</sub> is present in these conditions, the solutions involved in the experiments can be handled far more easily. Stoichiometric concentrations of THF and DIOX were not investigated in this study for two reasons: (i) THF at such a high concentration is not suitable for

our process equipment; (ii) in previous results obtained under batch conditions with a CO<sub>2</sub>/CH<sub>4</sub> gas mixture (Ricaurte et al., 2014a), the total quantity of gas enclathrated in hydrates was found to be much lower at the stoichiometric concentration than at a lower concentration (e.g., 4 wt% in water).

Fig. 6 shows the variation of the reactor pressure and temperature over time for the experiments carried out using the aqueous solution composed of (a) pure water, (b) water+SDS, (c) water+THF, and (d) water+DIOX, with snapshots of the bulk taken just before the reactor temperature was increased for dissociation. For the water+THF+SDS and water+DIOX+SDS systems, the following are presented in Figs. 7 and 8: evolution of the reactor pressure and temperature over time, the corresponding *P-T* diagram (only one experiment is shown for the sake of clarity), and snapshots taken during the hydrate formation. Table 4 contains all the relevant analytic and quantitative information for all the systems studied. Note that the values shown represent the arithmetic average values associated with the corresponding standard deviations (when several experiments are considered).

Comparing the trends obtained in Figs. 6-8, it is clearly apparent that two different system behaviors occur: (i) when THF and DIOX are mixed with SDS a dramatic decrease in the reactor pressure is observed during the experiment, and the pressure finally stabilizes at a constant value before dissociation begins; (ii) in the experiments where only one type of additive (i.e., DIOX, THF or SDS) is used, or none, the reactor pressure decreases very slowly at a quasi constant rate until the temperature has climbed back up to its initial value for dissociation. Note that the presence of 0.3 wt% SDS has no

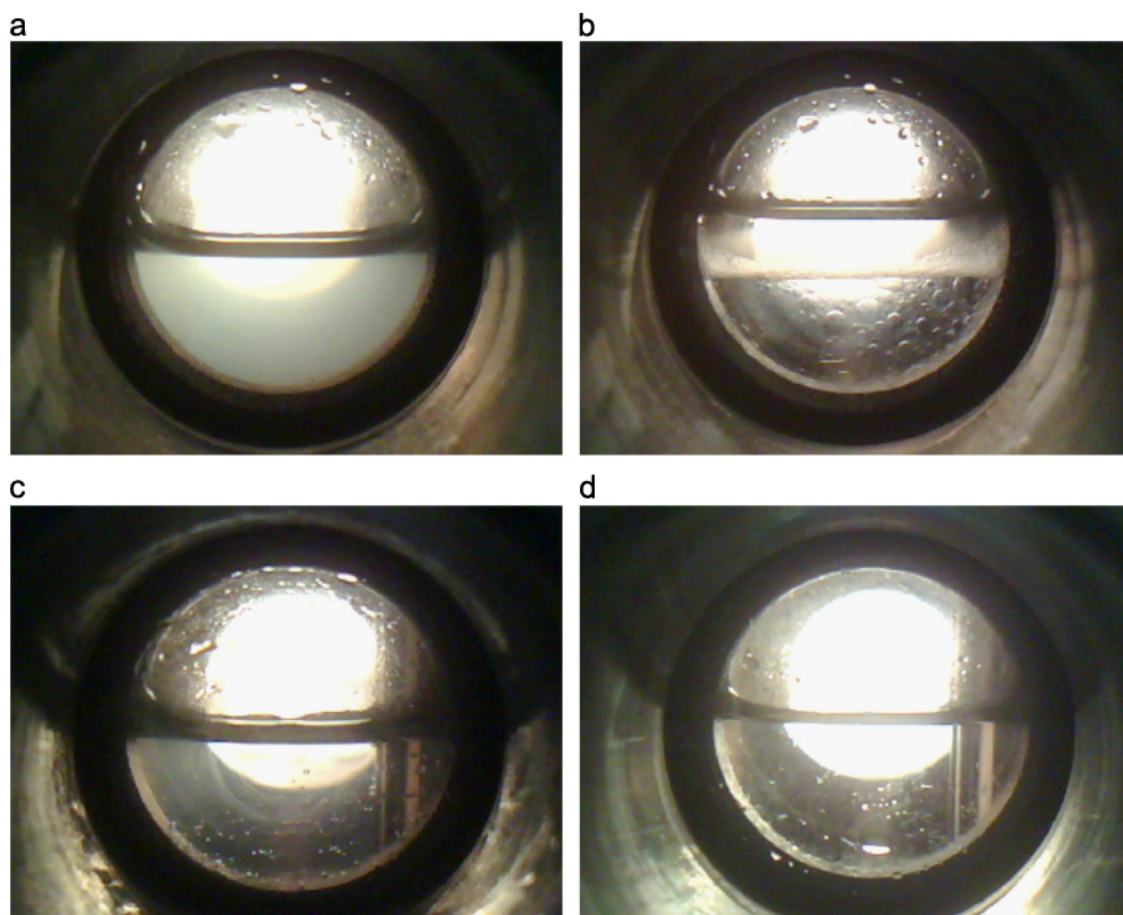
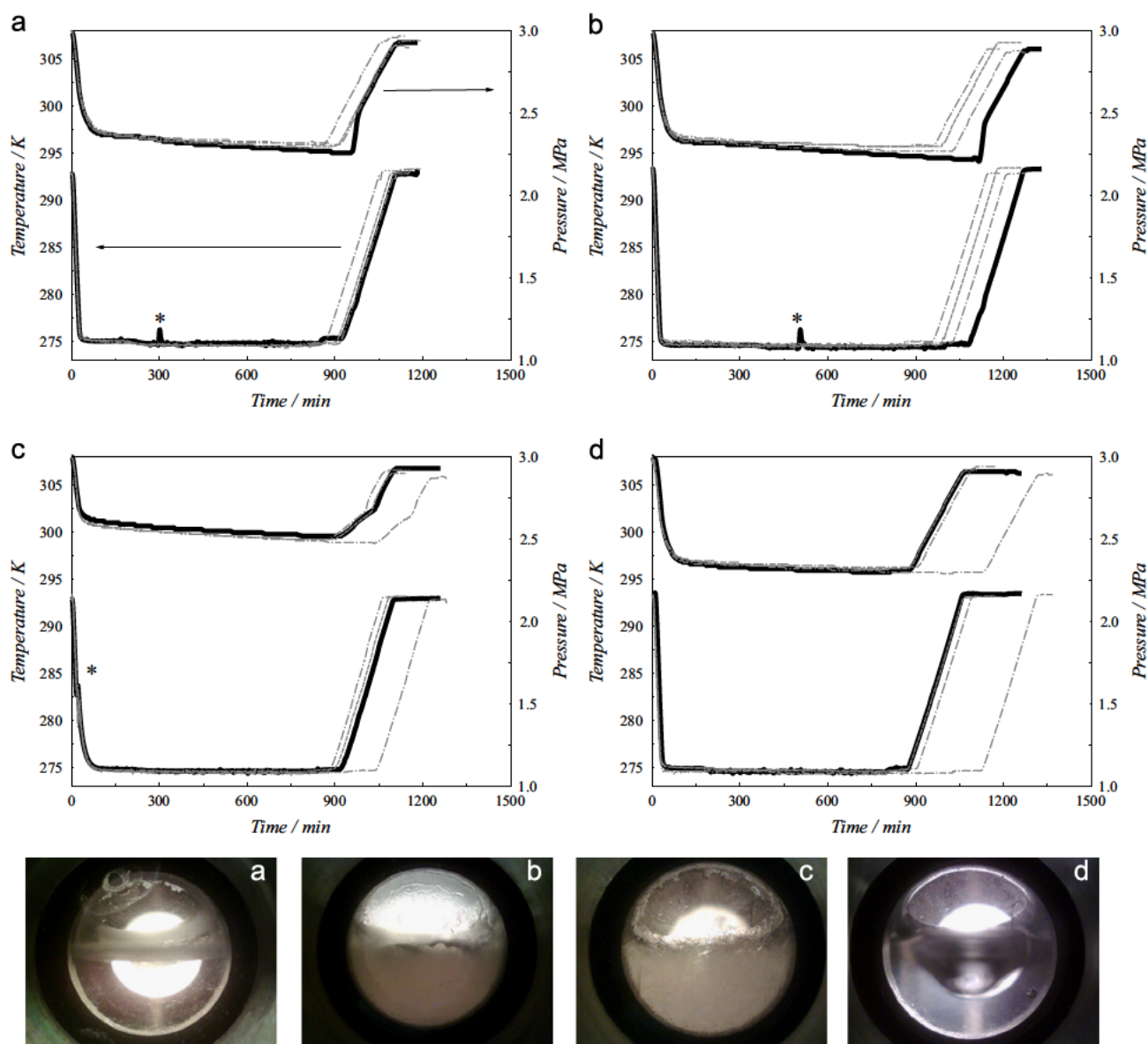


Fig. 5. Snapshots of solutions of organic additives at stoichiometric concentrations for (sII) hydrate formation in presence of CO<sub>2</sub> at 3.0 MPa. The agitation was stopped for taking the pictures. [THF] 19.6 wt%; [DIOX] 19.2 wt%; *T* 293 K. (a) H<sub>2</sub>O+THF: initial state before CO<sub>2</sub> pressurization; (b) H<sub>2</sub>O+THF+CO<sub>2</sub>: 30 min after CO<sub>2</sub> solubilization (no sensible change after 24 h); (c) H<sub>2</sub>O+DIOX initial state before CO<sub>2</sub> pressurization; (d) H<sub>2</sub>O+DIOX+CO<sub>2</sub>: 24 h after CO<sub>2</sub> solubilization.



**Fig. 6.** Experimental data of hydrate formation from aqueous solutions containing a single type of additive (no additive combination). Reactor pressure and temperature over time with: (a) only water (no additive); (b) water+0.3 wt% of SDS; (c) water+4 wt% of THF; (d) water+4.1 wt% of DIOX. 4 experiments were done for each system. The asterisk symbol \* shows the temperature peak produced by the hydrate crystallization.

measurable influence on the hydrate equilibrium conditions (Torré et al., 2012).

With pure water, or water+SDS, hydrate forms during only one experiment out of the four carried out in each case. When crystallization effectively occurs, the hydrate formation can easily be identified by a sudden increase in the reactor temperature pointed out by the single asterisk in Fig. 6(a) and (b). At these pressure and temperature conditions, the operating point is located in the hydrate region. As no thermodynamic promoter is present here, the hydrate which has crystallized at this temperature is unambiguously the  $\text{CO}_2$  hydrate. In addition, observation of the reactor interior reveals interesting details: as shown in the corresponding snapshot of Fig. 6(a), when no additive is used a crust is formed at the water-gas interface, and is likely to prevent the  $\text{CO}_2$  diffusing from the gas to the water. When SDS is added to water see snapshot of Fig. 6(b) the liquid/gas interface appeared to be covered by a hydrate layer and a thin layer of a solid was observed to be deposited on the reactor windows (note that due to the turbid aspect of the solution, it is not possible at this point to clearly distinguish whether hydrates are also present in the

bulk). In a previous study (Ricaurte et al., 2013), we estimated assuming ambient pressure conditions and the same surfactant concentration (i.e., 0.3 wt%) the Krafft temperature of the SDS at  $289 \pm 1$  K, which agrees with the value of  $285 \pm 4$  K proposed by Watanabe et al. (2005). Therefore, the turbidity observed at the hydrate forming temperature ( $T_{\text{avg}} = 274.6 \pm 0.2$  K) with SDS solutions (no other additive present) is due to the precipitation of the surfactant, as the solution is maintained at a temperature several Kelvins below the Krafft temperature of the SDS.

If we now consider the THF+SDS system, the sudden temperature increase of several Kelvins measured during the cooling phase of the reactor (peak signaled by a single asterisk in Fig. 7) is the exothermic signature of a hydrate crystallization. In this case, hydrates crystallize in the whole bulk, as proven in the snapshots of Fig. 7. In the  $P-T$  diagram presented in Fig. 7(b), since this crystallization point is located between the equilibrium curves of pure  $\text{CO}_2$  and mixed THF+ $\text{CO}_2$  hydrates, this formation is logically attributed to the THF+ $\text{CO}_2$  mixed hydrate. Then, when the system crosses over the  $\text{CO}_2$  hydrate equilibrium curve (i.e., it enters the



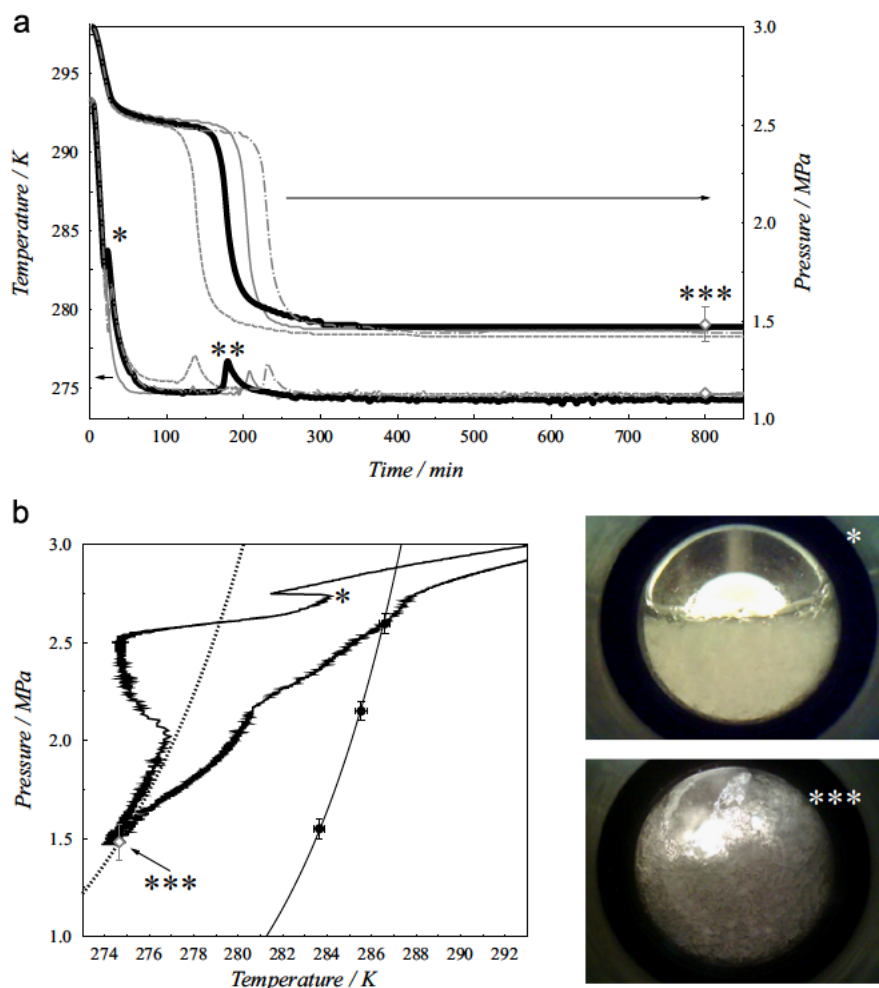


Fig. 7. Experimental data for the system THF+SDS with 4 wt% of THF and 0.3 wt% of SDS (4 experiments). (a) Evolution of the reactor pressure and temperature over time; (b)  $P$ - $T$  diagram for the experiment shown with a bold solid line in figure (a). The symbols \* and \*\* shows the two successive hydrate crystallisations. The snapshots corresponds to times identified by the symbols \* and \*\* on the plots. On the  $P$ - $T$  diagram: the regular solid line correspond to the mixed hydrate equilibrium curve drawn with the experimental data from Table 2 (full circles), the dotted line represented the  $\text{CO}_2$  hydrate equilibrium calculated with the CSMGem program (Sloan and Koh, 2008); the empty diamond is the theoretical equilibrium pressure calculated with CSMGem at the final experimental temperature (error bar is from the temperature uncertainty).

$\text{CO}_2$  hydrate stability zone), the presence of this mixed hydrate coupled with the surfactant triggers the formation of the  $\text{CO}_2$  hydrate, leading to a rapid drop in the reactor pressure. For the following, it is important to mention that the hydrate formation kinetics considered here is that of the pure  $\text{CO}_2$  hydrate, which takes place (in the  $\text{CO}_2$  hydrate stability zone) at an average temperature of  $274.6 \pm 0.2$  K. Note that, at this stage, the mixed hydrate (i.e., a  $\text{CO}_2$ +THF hydrate in that case) is already formed into the bulk, and we assume no thermodynamic effect of the thermodynamic promoter on this kinetics (as the organic compound has been consumed in the first crystallization).

Simultaneously with the  $\text{CO}_2$  enclathration, the temperature of the liquid phase again increases by several Kelvins. The hydrate formation ends when the reactor pressure becomes equal to the  $L_w$   $H$   $V$  equilibrium point of the  $\text{CO}_2$  hydrate, as it is strongly corroborated by the theoretical equilibrium point calculated using the CSMGem program (Sloan and Koh, 2008). It is also worth noting from Table 4 that the time when the enclathration rate is at its maximum ( $t_{(dn/dt)|_{\max}} = 187 \pm 39$  min) coincides with the maximum temperature measured, the latter peak being due to the hydrate crystallization ( $t_2 = 189 \pm 40$  min). Finally, the pressure associated with the maximum enclathration rate was found to be nearly constant and equal to  $2.05 \pm 0.03$  MPa. The determination of this value can be very useful for improving the kinetic performance of a hydrate based contactor working in a semi continuous mode (Torré

et al., 2012). Interestingly, when THF is added to the water (see Fig. 6 (c)) the formation of the mixed THF+  $\text{CO}_2$  hydrate occurs a relatively short time  $24 \pm 4$  min after the reactor begins to cool, leading to a sudden increase in the bulk temperature by several Kelvins (shown by the single asterisk in Fig. 6(c)). As this time is comparable to the one obtained for THF+SDS ( $23 \pm 4$  min), it can be concluded that the presence of the surfactant in the solution does not reduce the time needed for the first crystallization to develop. Thus, THF used alone does not, under these conditions, enhance the rate of  $\text{CO}_2$  consumption (compared to the two additives being used in combination). This last result is in agreement with a previous one (Ricaurte et al., 2013) obtained with a  $\text{CO}_2/\text{CH}_4$  gas mixture instead of pure  $\text{CO}_2$ .

With the DIOX+SDS system, similar global tendencies are observed as for the THF+SDS system. Again, a good reproducibility of the general behavior is obtained as all runs result in two successive crystallizations, which are indicated by a single and a double asterisk in Fig. 8(a). The first hydrate formation is measured as taking much longer than with the THF+SDS system: an average value of  $120 \pm 38$  min is obtained for the DIOX+SDS system, compared to only  $23 \pm 4$  min for THF+SDS. There is a satisfactory explanation for this slowness: the fact that DIOX has a weaker thermodynamic promoting effect, as it was clearly demonstrated previously by the analysis of the results plotted in Fig. 4. By analogy with the THF+SDS case, and in spite of the fact that the first crystallization point is located inside the  $\text{CO}_2$  hydrate stability

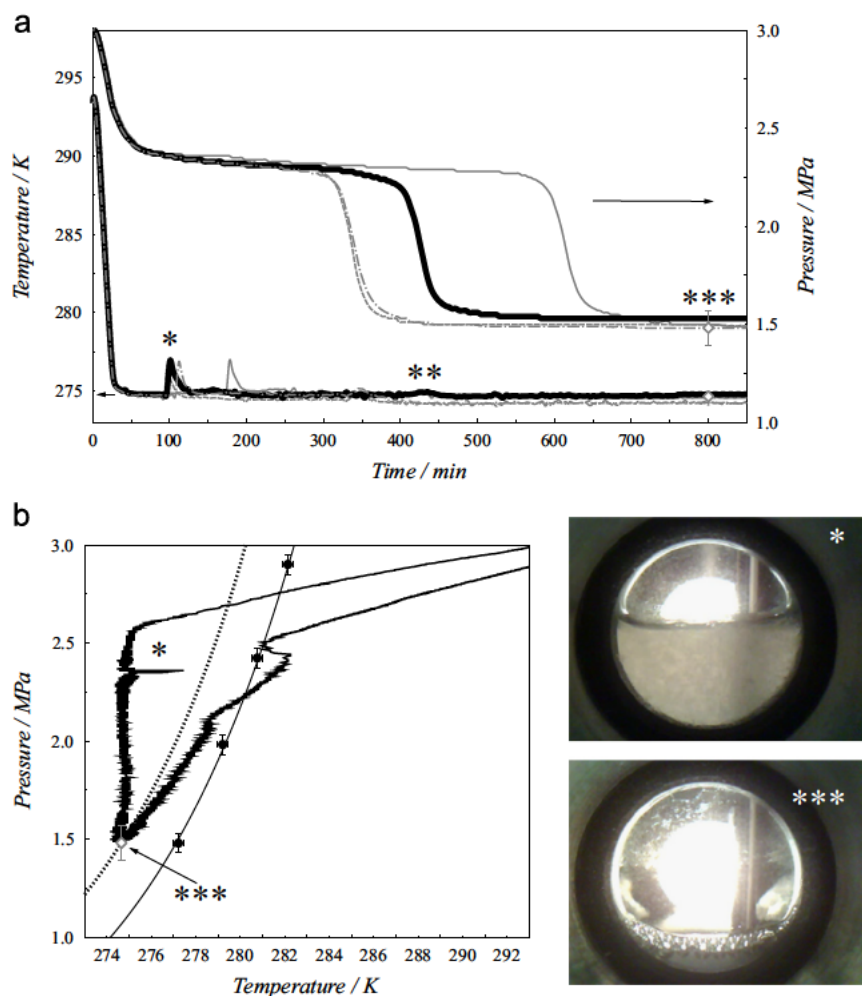


Fig. 8. Experimental data for the system DIOX+SDS with 4.1 wt% of DIOX and 0.3 wt% of SDS (4 experiments). (a) Evolution of the reactor pressure and temperature over time; (b)  $P$ - $T$  diagram for the experiment shown with a bold solid line in figure (a). The symbols \* and \*\*\* shows the two successive hydrate crystallisations. The snapshots corresponds to times identified by the symbols \* and \*\*\* on the plots. On the  $P$ - $T$  diagram: the regular solid line correspond to the mixed hydrate equilibrium curve drawn with the experimental data from Table 3 (full circles), the dotted line represented the  $\text{CO}_2$  hydrate equilibrium calculated with the CSMGem program (Sloan and Koh, 2008); the empty diamond is the theoretical equilibrium pressure calculated with CSMGem at the final experimental temperature (error bar is from the temperature uncertainty).

Table 4

Kinetics analytical information corresponding to the various systems studied for  $T_{\text{avg}}$  of  $274.6 \pm 0.2$  K.  $t_1$  is the time of mixed hydrate formation;  $t_2$  is the time for pure  $\text{CO}_2$  hydrate formation; the total mol number of  $\text{CO}_2$  captured is considered  $t = 800$  min. Four experiments were done for each system studied.

| System studied | Hydrates? (for 4 exp.) | $t_1$ (min)  | $t_2$ (min)   | $n_{\text{CO}_2}^{\text{capt}}$ (mol ( $\times 10^2$ )) | $t_{90\%}$ (min) | $(dn/dt) _{\text{max}}$ (mol min <sup>-1</sup> ( $\times 10^3$ )) | $t_{(dn/dt) _{\text{max}}}$ (min) | $P_{(dn/dt) _{\text{max}}}$ (MPa) |
|----------------|------------------------|--------------|---------------|---|------------------|---|-----------------------------------|-----------------------------------|
| Pure water     | Yes (1/4)              | -            | 300           | 5.4   | -                | -   | -                                 | -                                 |
|                | No (3/4)               | -            | -             | $5.3 \pm 0.1$   | -                | -   | -                                 | -                                 |
| Only SDS       | Yes (1/4)              | -            | 505           | 5.6   | -                | -   | -                                 | -                                 |
|                | No (3/4)               | -            | -             | $5.4 \pm 0.1$   | -                | -   | -                                 | -                                 |
| Only THF       | Yes (4/4)              | $24 \pm 4$   | -             | $3.9 \pm 0.1$   | -                | -   | -                                 | -                                 |
| Only DIOX      | No (4/4)               | -            | -             | $5.2 \pm 0.1$   | -                | -   | -                                 | -                                 |
| SDS+THF        | Yes (4/4)              | $23 \pm 4$   | $189 \pm 40$  | $10.7 \pm 0.1$  | $206 \pm 37$     | $2.9 \pm 0.2$   | $187 \pm 39$                      | $2.05 \pm 0.03$                   |
| SDS+DIOX       | Yes (4/4)              | $120 \pm 38$ | $440 \pm 130$ | $10.4 \pm 0.1$  | $444 \pm 131$    | $1.2 \pm 0.1$   | $431 \pm 130$                     | $1.87 \pm 0.02$                   |

zone for the DIOX+SDS system, we suppose that the formation mechanism remains identical for the two ethers: first, the mixed hydrate DIOX+ $\text{CO}_2$  crystallizes first, and then the pure  $\text{CO}_2$  hydrate forms later. Concerning the hydrate formation rate, the maximum value obtained with DIOX+SDS is  $\sim 2.4$  less than with THF+SDS, with  $t_{90\%}$  values much higher than for THF (compared to the system THF+SDS, it takes about twice as long to capture 90% of the total quantity of  $\text{CO}_2$  using the DIOX+SDS system). Again, the pressure associated with the maximum enclathration rate was nearly constant, but slightly lower for DIOX+SDS

( $1.87 \pm 0.02$  MPa) compared to THF+SDS. Finally, the system stabilizes at the same triphasic i.e., the liquid hydrate vapor ( $L_w$  H V)  $\text{CO}_2$  hydrate equilibrium point as with THF+SDS. Surprisingly, when only DIOX was used (see Fig. 6(d)), no crystallization was observed for the four experiments carried out. This behavior demonstrates that the presence of the surfactant in the solution is of paramount importance for achieving  $\text{CO}_2$  enclathration at a high rate. Therefore, the DIOX+SDS combination appears less advantageous than THF+SDS in terms of induction time (time to crystallize the first hydrate), and also in terms

of the overall kinetics if we look at parameters such as the maximum enclathration rate and the time to reach the  $L_w H V$  equilibrium value.

Interestingly, observation showed that the hydrates visible through the reactor windows for the THF+SDS and DIOX+SDS systems had very different morphologies. In Figs. 7 and 8, the snapshot shown by a single asterisk was taken just after the first hydrate crystallization, and the one indicated by a triple asterisk was taken just before the dissociation. With the THF+SDS system (Fig. 7), it is clear that the first crystals formed in the whole bulk and then others grew along the sapphire surface. With the DIOX+SDS system (Fig. 8), the first crystallization also occurs in the bulk, but there is almost no growth of crystals on the reactor windows. This observation was made in every one of the experiments carried out with these two systems. One can assume that if a difference of hydrate growth on the walls applies to the whole reactor, it can significantly influence the hydrate formation kinetics. One assumption, to explain the enclathration performance observed for systems with kinetic promoters in quiescent conditions, postulates that a porous medium forms on the reactor walls by progressive aggregation of small hydrate particles. If the network of hydrates formed can be wetted by the solution, the liquid is sucked by capillarity through the porous structure, and the hydrate formation can be qualified as "capillary driven". This mechanism has been already discussed and shown visually (Gayet et al., 2005; Zhang and Lee, 2009) and is in close relationship with the adsorption of surfactants on hydrates (Aman et al., 2013; Lo et al., 2010). Differences in the physico chemical properties of the systems studied (e.g., THF+SDS and DIOX+SDS) such as the adhesion force between the hydrate(s) and sapphire, or the wettability of the hydrate/solution toward the process materials may significantly impact the capillary driven mechanism and could explain the differences in the kinetic performance of these combination of additives.

## 5. Conclusions and prospects

The search for THF substitutes to enhance hydrate formation is an important goal, both for fundamental investigations and for practical applications, as it is hardly conceivable that large quantities of THF could be used in the future if hydrate based processes have to be scaled up at industrial level.

From a practical point of view, DIOX should be chosen in preference to THF as the former is less toxic, less volatile, and much less aggressive to process equipment. Interestingly, at high concentrations (e.g., ~20 wt% in water) and with CO<sub>2</sub> at 3.0 MPa, a DIOX water solution does not separate into two liquid phases at ambient temperature (293 K), contrarily to the water+THF system. However, for the same concentrations of organic additives in water, the mixed hydrate THF+CO<sub>2</sub> is formed at higher temperature and lower pressure than the DIOX+CO<sub>2</sub> mixed hydrate. Therefore, using CO<sub>2</sub> as guest, the respective positions of the  $L_w H V$  equilibrium curves demonstrate unambiguously that THF is a better thermodynamic hydrate promoter than DIOX.

If a low concentration of thermodynamic promoter is used, the global hydrate formation mechanism could be summarized in the two following steps: (i) a mixed hydrate (i.e., THF+CO<sub>2</sub> or DIOX+CO<sub>2</sub>) first crystallizes into the bulk, and (ii) this mixed hydrate triggers, when SDS is present, the formation of the pure CO<sub>2</sub> hydrate and influences its kinetics. Concerning the CO<sub>2</sub> hydrate formation kinetics, only the use of a combination of THF or DIOX together with the anionic surfactant SDS yields a high rate of CO<sub>2</sub> consumption. Therefore, THF (used in combination to SDS) as a hydrate promoter still appears most favorable in the scope of this work performed with CO<sub>2</sub>, from a kinetic standpoint. Nevertheless, due to the very advantageous and user friendly qualities of DIOX

(compared to THF), DIOX remains attractive in practical applications if moderate promoting effects are satisfactory.

The reason why these combinations of additives are so efficient is not yet fully understood. However, some of our observations suggest that physico chemical parameters (such as the adhesion force between hydrates and/or with the process materials, and/or the wettability of the aqueous solution toward the same) play an important role in the kinetic promotion effects. We believe that factors linked to the "capillary driven" mechanism in which the solution is pumped through a porous medium formed by the aggregation of hydrate particles on the reactor walls are of paramount importance. The formation of this porous hydrate structure may be directly correlated with an anti agglomerant effect of SDS on the CO<sub>2</sub>, and THF+CO<sub>2</sub> or DIOX+CO<sub>2</sub> mixed hydrates. However, this last point has not been clearly demonstrated to date. Understanding the role of the surfactant in the action mechanism, as well as the influence of the crossed interactions between the surfactant and the thermodynamic promoter, calls for further experiments which are currently in progress in our laboratory.

## Acknowledgments

We would like to extend warm thanks to the staff of the "Atelier de Physique" and J. Diaz from the University of Pau for their valuable technical work. Also, we appreciatively acknowledge the support of the Carnot Institute ISIFoR.

## Appendix A. Supporting information

Supplementary data associated with this article can be found in the online version at <http://dx.doi.org/10.1016/j.ces.2015.01.018>.

## References

- Ahmad, N., Phillips, W.A., 1987. Thermal conductivity of ice and ice clathrate. *Solid State Commun.* 63 (2), 167–171.
- Aman, Z.M., Olcott, K., Pfeiffer, K., Sloan, E.D., Sum, A.K., Koh, C.A., 2013. Surfactant adsorption and interfacial tension investigations on cyclopentane hydrate. *Langmuir* 29 (8), 2676–2682.
- Anderson, R., Chapoy, A., Tohidi, B., 2007. Phase relations and binary clathrate hydrate formation in the system H<sub>2</sub>-THF-H<sub>2</sub>O. *Langmuir* 23, 3440–3444.
- Andersson, P., Ross, R.G., 1983. Effect of guest molecule size on the thermal conductivity and heat capacity of clathrate hydrates. *J. Phys. C: Solid State Phys.* 16 (8), 1423–1432.
- Arnett, E.M., Tompson, F.M., Zare, R.M., 1995. *Prudent Practices in the Laboratory: Handling and Disposal of Chemicals*. National Academy Press, Washington, DC p. 1995.
- BASF, 2013. 1,3-Dioxolane. Commercial Brochure, 2013 ed. Provided by BASF [www.basf.com/performance-materials](http://www.basf.com/performance-materials).
- de Deugd, R.M., Jager, M.D., de Swaan Arons, J., 2001. Mixed hydrates of methane and water-soluble hydrocarbons modeling of empirical results. *AIChE J.* 47 (3), 693–704.
- Delahaye, A., Fournaison, L., Marinhas, S., Chatti, I., 2006. Effect of THF on equilibrium pressure and dissociation enthalpy of CO<sub>2</sub> hydrates applied to secondary refrigeration. *Ind. Eng. Chem. Res.* 45 (1), 394–397.
- Delahaye, A., Fournaison, L., Marinhas, S., Martínez, M.C., 2008. Rheological study of image hydrate slurry in a dynamic loop applied to secondary refrigeration. *Chem. Eng. Sci.* 63 (13), 3551–3559.
- Dicharry, C., Duchateau, C., Asbai, H., Broseta, D., Torrè, J.-P., 2013. Carbon dioxide gas hydrate crystallization in porous silica gel particles partially saturated with a surfactant solution. *Chem. Eng. Sci.* 98 (19), 88–97.
- Eslamimanesh, A., Mohammadi, A.H., Richon, D., Naidoo, P., Ramjugernath, D., 2012. Application of gas hydrate formation in separation processes: a review of experimental studies. *J. Chem. Thermodyn.* 46, 62–71.
- Gayet, P., Dicharry, C., Marion, G., Graciaa, A., Lachaise, J., Nesterov, A., 2005. Experimental determination of methane hydrate dissociation curve up to 55 MPa by using a small amount of surfactant as hydrate promoter. *Chem. Eng. Sci.* 60, 5751–5758.
- Jeffrey, G.A., 1984. Hydrate inclusion compounds. *J. Inclusion Phenom.* 1, 211–222.
- Kang, S.-P., Lee, H., Lee, C.-S., Sung, W.-M., 2001. Hydrate phase equilibria of the guest mixtures containing CO<sub>2</sub>, N<sub>2</sub> and Tetrahydrofuran. *Fluid Phase Equilib.* 185, 101–109.

- le Parlouër, P., Dalmazzone, C., Herzhaft, B., Rousseau, L., Mathonat, C., 2004. Characterisation of gas hydrates formation using a new high pressure Micro-DSC. *J. Therm. Anal. Calorim.* 78, 165–172.
- Lee, Y.-J., Kawamura, T., Yamamoto, Y., Yoon, J.-H., 2012. Phase equilibrium studies of tetrahydrofuran (THF)+CH<sub>4</sub>, THF+CO<sub>2</sub>, CH<sub>4</sub>+CO<sub>2</sub>, and THF+CO<sub>2</sub>+CH<sub>4</sub> hydrates. *J. Chem. Eng. Data* 57 (12), 3543–3548.
- Lirio, C.F.S., Pessoa, F.L.P., Uller, A.M.C., 2013. Storage capacity of carbon dioxide hydrates in the presence of sodium dodecyl sulfate (SDS) and tetrahydrofuran (THF). *Chem. Eng. Sci.* 96 (7), 118–123.
- Lo, C., Zhang, J.S., Couzis, A., Somasundaran, P., Lee, J.W., 2010. Adsorption of cationic and anionic surfactants on cyclopentane hydrates. *J. Phys. Chem. C* 114, 13385–13389.
- Maekawa, T., 2013. Equilibrium conditions of clathrate hydrates formed from xenon and aqueous solutions of acetone, 1,4-dioxane and 1,3-dioxolane. *Fluid Phase Equilib.* 339, 15–19.
- Martinez, M.C., Dalmazzone, D., Fürst, W., Delahaye, A., Fournaison, L., 2008. Thermodynamic properties of THF+CO<sub>2</sub> hydrates in relation with refrigeration applications. *AIChE J.* 54 (4), 1088–1095.
- Makino, T., Sugahara, T., Ohgaki, K., 2005. Stability boundaries of tetrahydrofuran-water system. *J. Chem. Eng. Data* 50, 2058–2060.
- Mackison, F.W., Stricoff, R.S., Partridge, L.J., 1981. Occupational Health Guidelines for Chemical Hazards. U.S. Government Printing Office, Washington, DC p. 2 (Publication No. 81-123).
- Nakayama, H., Hashimoto, M., 1980. Hydrates of organic compounds. V. The clathrate hydration of alcohols. *Bull. Chem. Soc. Jpn.* 53, 2427–2433.
- NFPA (National Fire Protection Association), 2010. Fire Protection Guide to Hazardous Materials, 14th ed. Quincy, MA 2010.
- NFPA (National Fire Protection Association), 2002. Fire Protection Guide to Hazardous Materials, 13th ed. Quincy, MA 2002.
- Peng, D.Y., Robinson, D.B., 1976. A new two-constant equation of state. *Ind. Eng. Chem. Fundam.* 15 (1), 59–64.
- Ricaurte, M., Dicharry, C., Broseta, D., Renaud, X., Torrè, J.-P., 2013. CO<sub>2</sub> removal from a CO<sub>2</sub>-CH<sub>4</sub> gas mixture by clathrate hydrate formation using THF and SDS as water-soluble hydrate promoters. *Ind. Eng. Chem. Res.* 52, 899–910.
- Ricaurte, M., Dicharry, C., Renaud, X., Torrè, J.-P., 2014a. Combination of surfactants and organic compounds for boosting CO<sub>2</sub> separation from natural gas by clathrate hydrate formation. *Fuel* 122 (15), 206–217.
- Ricaurte, M., Torrè, J.-P., Asbai, A., Broseta, D., Dicharry, C., 2012. Experimental data, modeling and correlation of carbon dioxide solubility in aqueous solutions containing low concentrations of clathrate hydrate promoters: application to CO<sub>2</sub>-CH<sub>4</sub> gas mixtures. *Ind. Eng. Chem. Res.* 51, 3157–3169.
- Ricaurte, M., Torrè, J.-P., Diaz, J., Dicharry, C., 2014b. In-situ injection of THF to trigger gas hydrate crystallization: application to the evaluation of a kinetic hydrate promoter. *Chem. Eng. Res. Des.* 92, 1674–1680.
- Shin, H.J., Lee, Y.-J., Im, J.-H., Won Han, K., Lee, J.-W., Lee, Y., Dong Lee, J., Jang, W.-Y., Yoon, J.-H., 2009. Thermodynamic stability, spectroscopic identification and cage occupation of binary CO<sub>2</sub> clathrate hydrates. *Chem. Eng. Sci.* 64, 5125–5130.
- Sloan, E.D., 2003. Fundamental principles and applications of natural gas hydrates. *Nature* 426, 353–363.
- Sloan, E.D., Koh, C.A., 2008. Clathrate Hydrates of Natural Gases, third ed. CRC Press, New York, NY.
- Torrè, J.-P., Ricaurte, M., Dicharry, C., Broseta, D., 2012. CO<sub>2</sub> enclathration in the presence of water-soluble hydrate promoters: hydrate phase equilibria and kinetic studies in quiescent conditions. *Chem. Eng. Sci.* 82, 1–13.
- Uchida, T., Wakakura, M., Miyake, A., Ogawa, T., 2008. Hazard evaluation for oxidation of cyclic ethers. *J. Therm. Anal. Calorim.* 93 (1), 247–251.
- Venkatesjvara, A., Easterfield, J.R., Davidson, D.W., 1967. A clathrate hydrate of 1,3-dioxolane. *Can. J. Chem.* 45, 884–886.
- Wang, L., Zhang, X., Li, H., Shao, L., Zhang, D., Jiao, L., 2013. Theory research on desalination of brackish water using gas hydrate method. *Adv. Mater. Res.* 616–618, 1202–1207.
- Watanabe, K., Imai, S., Mori, Y.H., 2005. Surfactant effects on hydrate formation in an unstirred gas/liquid system: an experimental study using HFC-32 and sodium dodecyl sulphate. *Chem. Eng. Sci.* 60, 4846–4857.
- Yang, M., Song, Y., Liu, W., Zhao, J., Ruan, X., Jiang, L., Li, Q., 2013. Effects of additive mixtures (THF/SDS) on carbon dioxide hydrate formation and dissociation in porous media. *Chem. Eng. Sci.* 90 (7), 69–76.
- Yonekura, T., Yamamuro, O., Matsuo, T., Suga, H., 1995. Calorimetric and DTA studies of 1,3-dioxolane hydrate and (1,3-dioxolane)<sub>x</sub>(tetrahydrofuran)<sub>x</sub> mixed hydrates. *Thermochim. Acta* 266, 65–77.
- Zhang, J., Lee, J.W., 2009. Enhanced kinetics of CO<sub>2</sub> hydrate formation under static conditions. *Ind. Eng. Chem. Res.* 48, 5934–5942.
- Zhong, D.L., Daraboina, N., Englezos, P., 2013. Recovery of CH<sub>4</sub> from coal mine model gas mixture (CH<sub>4</sub>/N<sub>2</sub>) by hydrate crystallization in the presence of cyclopentane. *Fuel* 106, 425–430.